Optical tweezers for force measurements on DNA in nanopores

U. F. Keyser,[a] J. van der Does, C. Dekker, and N. H. Dekker[b]
Kavli Institute of Nanoscience, Delft University of Technology, Lorentzweg 1, 2628 CJ Delft, The Netherlands

(Received 2 August 2006; accepted 6 September 2006; published online 26 October 2006)

We demonstrate the means to integrate two powerful and widely used single-molecule techniques, viz., optical tweezers and solid-state nanopores. This setup permits simultaneous spatial sampling and high-resolution force measurements of nucleic acids and proteins. First, we demonstrate the rapid spatial localization of nanopores using our custom-built inverted microscope and ionic current measurements. This is made possible by including a specialized flow cell for silicon-based nanopores with an optical window for a high-numerical aperture microscope. Subsequently, we can insert individual DNA molecules into a single nanopore and arrest the DNA during voltage-driven translocation. To detect the position of the trapped particle in the optical trap with high accuracy in the presence of the nanopore, the optical tweezers uses reflected light from the bead for detection. Consequently, we can use our setup to directly determine the force on a DNA molecule in a solid-state nanopore. Finally, we suggest a number of new experiments that become possible with this unique technique. © *2006 American Institute of Physics.* [DOI: 10.1063/1.2358705]

I. INTRODUCTION

The demonstration of protein nanopores as molecular Coulter counters for nanometer-sized objects like ribonucleic acid (RNA)[1] or deoxyribonucleic acid (DNA)[2] has inspired the fabrication of single nanopores in insulating membranes.[3,4] These nanopores could serve as basic building blocks in future lab-on-a-chip technology. Despite the great experimental interest, two main questions remained yet unsolved: (i) how can one measure the absolute position of a biopolymer such as DNA or RNA in the nanopore and control, slow down, or even arrest the voltage-driven translocation, and (ii) what is the magnitude of the forces acting on DNA molecules inside the nanopore during this voltage-driven process?

The first question is of great technological interest. One drawback of the experiments published so far is the lack of a ruler that can tell the position of the translocating biomolecule, like DNA, RNA, or a protein, in the nanopore. This is true for translocation through both protein and solid-state nanopores. With an absolute position measurement, detecting specific sequences of DNA or RNA or binding sites for proteins appears to be possible. A length scale could be implemented by attaching markers to known sequences in the translocating DNA molecules, but this approach is severely limited by the spatial resolution of ~300 nm obtained with the ionic current technique.[5] The main reason for this limitation is the high translocation speed of the DNA. The speed could in principle be set to any value and the translocation could even be arrested if a nonelectrical, opposing force was applied to one end of the DNA molecule. This would allow for long-time averaging of the ionic current measurements combined with exact positioning of the DNA in the nanopore and dramatically increase the resolution compared to freely translocating molecules, which might be important for DNA sequencing.

The second question, concerning the magnitude of the voltage-generated forces acting on DNA in a nanopore, has never been directly answered. Knowing the magnitude of the force would give insight into the mobility of ions around the DNA and the nanopore walls. A prediction of the force is complicated since the effective charge of DNA depends on the experimental conditions, see, e.g., Refs. 6–10. The uncertainty stems from the fact that the distribution and mobility of the counterions on the DNA molecule are not really known. We demonstrate here that our novel method allows measuring the force on a single DNA molecule in a nanopore.

In this paper we describe a novel experimental apparatus that can address both these technological and physics questions. We designed optical tweezers[11,12] that are integrated with high-resolution ionic current detection. Using the new combination of two powerful single-molecule techniques (optical tweezers and nanopores), we are able to controllably insert a single DNA molecule into a solid-state nanopore. The electrical force exerted on the DNA coupled to a polystyrene bead is measured with the optical trap. We exert complete control over the position and translocation speed of the DNA in this configuration. This will allow exciting future experiments in the field of biophysics, such as detecting protein binding sites[13] and forces, or unraveling the secondary structure of RNA.[14,15]

The paper is organized into several sections. First we will briefly discuss the fabrication of nanopores, followed by a description of the optical tweezers and the data acquisition. Afterwards we describe the custom-built sample cell that

[a]Present address: Institut für Experimentelle Physik I, Universität Leipzig, Germany.
[b]Author to whom correspondence should be addressed; electronic mail: N.H.Dekker@tudelft.nl

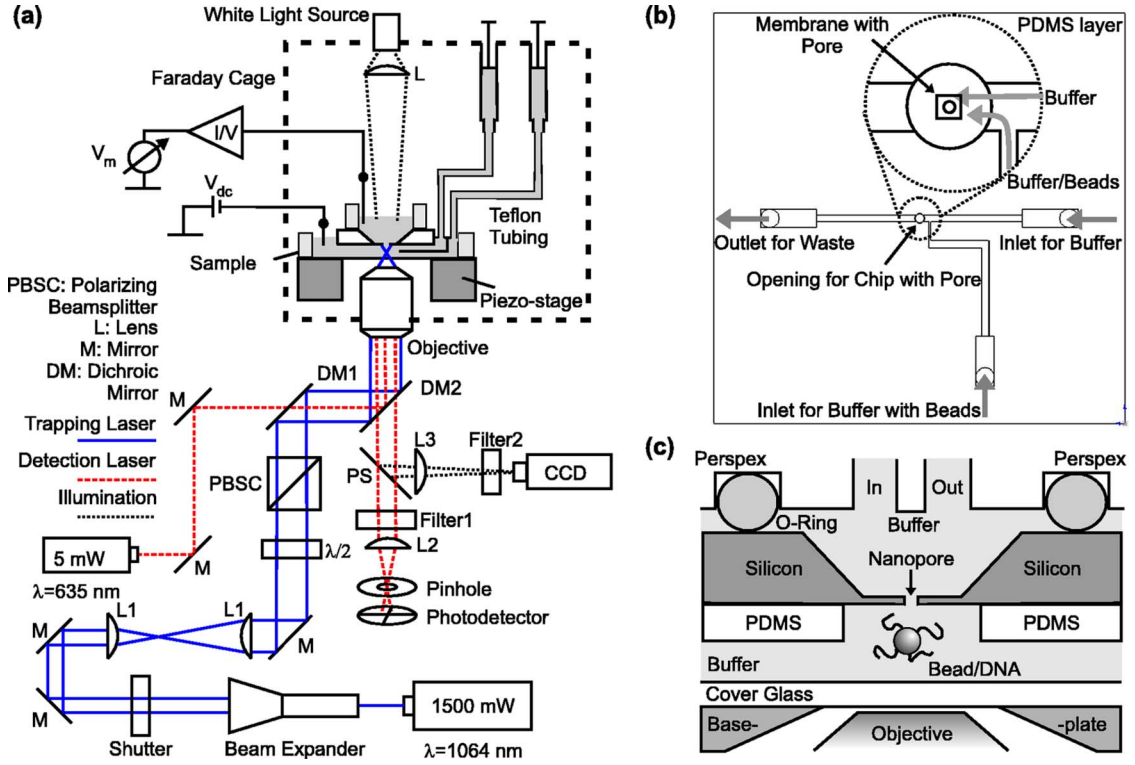

FIG. 1. (Color online) (a) Experimental configuration of the optical tweezers setup with the ionic current detection. The setup is based on a custom-built inverted microscope. The path of the infrared laser is shown blue and the path of the red laser is shown in red. The position detection is done with the red light reflected by the bead. A small Faraday cage (indicated by thick dashed lines) is used to shield the setup from interfering electromagnetic signals and is mounted onto micrometer stages used for coarse alignment (not shown). The sample is mounted on a three-axis piezoelectric stage for high-resolution positioning of the sample relative to the optical trap. (b) Outline of the PDMS layer of the sample cell, on the side closest to the objective. The two fluid inlets can be flushed with buffer and buffer with beads, respectively. The chip is mounted on top of the hole indicated in the center. The inset shows the position of the membrane with the nanopore with respect to the hole in the PDMS layer. The flow paths for the buffer and beads are shown by the arrows. (c) Cross section of the assembled flow cell (not to scale) showing the objective, baseplate (PEEK), cover glass, PDMS layer, nanopore chip, and top part (perspex). The buffer in the two reservoirs on both sides of the nanopore chip is shown in light gray. The seal on the top on the nanopore chip is established via an O-ring and on the bottom by the PDMS layer. Beads coated with DNA (see text) are held in the optical trap and moved relative to the nanopore.

permits measurements of the ionic current while including a window for optical access. Experiments that characterize the setup and the nanopores are described subsequently. Finally we demonstrate that we can insert a single DNA-molecule into a nanopore, completely arrest its translocation, and measure the force applied to it.

II. NANOPORES

Single solid-state nanopores are fabricated using standard semiconductor processing of silicon chips (4 mm × 8 mm, thickness 0.5 mm) that yield freestanding SiN membranes with 20 nm thickness. These are covered by sputtered silicon oxide with a thickness of 20 nm on each side, resulting in a membrane of total thickness of 60 nm. A transmission electron microscope (TEM) is used to drill the nanopores in the resulting membrane by sputtering of atoms from the layer by the tightly focused electron beam. The diameter of the nanopores is tuned by controlled electron-beam irradiation with lower intensity. This technique is extremely powerful because it allows monitoring the formation and tuning of the nanopores in real time with subnanometer resolution. Detailed descriptions and studies of this process, as well as the physical and surface characteristics of the nanopores, are published elsewhere.[4,16–18] A TEM image of a typical nanopore is shown in the inset of Fig. 2.

III. OPTICAL TWEEZERS

A schematic overview of our setup is shown in Fig. 1. For specificity, the important components in Fig. 1(a) are denoted below with the manufacturer's part numbers. Specifications for standard parts like mirrors or mirror holders are not included. The optical tweezers system is installed on a vibration isolation table (TMC). For the optical trapping we use a diode-pumped Nd:YAG laser system (1.5 W, CrystaLaser, ultrastable intensity, wavelength 1064 nm). The initial beam has a diameter of 0.45 mm ($1/e^2$) and is expanded by a beam expander (HEBX-4.0–10x1064, CVI Laser) and by a pair of lenses [L1 in Fig. 1(a), focal lengths 7.5 cm and 17.5 cm, Newport] to collimate the beam and overfill the back aperture of the objective. The beam passes through a half wave plate (10RP32–1064, Newport) and a polarizing beamsplitter cube (10BC16PC.9, Newport) to controllably attenuate the power.

We use a red diode laser (5 mW, Coherent, wavelength 635 nm) to detect the position of the trapped particles. We chose to base the detection system for the optical tweezers based on the reflected light from the bead[19] in order to maximize flexibility for the design of the sample cell containing the nanopore. The use of a single microscope objective with high numerical aperture instead of conventional approaches with two,[12] leaves the whole space on top of the objective

free for the flow cell. The red laser beam is coupled into the optical path by a dichroic mirror [DM1 in Fig. 1(a), SWP-45-Runp1064-Tunp633-PW-2025-C, CVI Laser]. Two mirrors are used to render the red laser collinear to the IR laser. A second, identical dichroic mirror [DM2 in Fig. 1(a), CVI Laser] reflects both beams into the objective (UPLAPO, 60×, water immersion, numerical aperture 1.2, Olympus). The objective is mounted on a very stable, custom-made, differential micrometer stage that allows movement along the optical axis with an accuracy better than 1.0 μm. The deviation perpendicular to the optical axis is less than 1.0 μm over the full travel range of 3 mm. All nonspecified mirrors are standard mirrors (Thorlabs) with broadband coating in the specific wavelength range.

The red light reflected from the bead in the optical trap is used for the detection of the bead position relative to the trap center. The light collected by the objective is focused by a tube lens [L2 in Fig. 1(a), $f=17.5$ cm, Newport] onto a pinhole for spatial filtering, as in confocal microscopy. The pinhole is mounted onto 3 micometer-screws for alignment perpendicular and along the optical axis (Newport). The spatial filtering with the pinhole enhances the resolution of the system by a factor of 2 because the detection of light reflected from surfaces other than the bead is reduced. The light transmitted through the pinhole is detected with a quadrant photodetector (PD) (Spot-4E, UDT-Sensors). The PD is protected from stray light by a narrow laser-line filter ($\lambda_{center}=635$ nm, Thorlabs). The PD is also mounted onto 3 micometer-screws (Newport) to center the light reflected by the bead.

Due to the low intensity of the reflected light, the voltage signals from the four quadrants of the PD are each amplified by a custom-made preamplifier with a bandwidth of 250 kHz. The position information is obtained with a commercial amplifier for quadrant PDs (OD-301, Ontrak) with a typical bandwidth of 15 kHz. A digital-to-analog converter (PCI-6036E, National Instruments) is used to measure the analog voltage signals from the amplifiers. For imaging and coarse alignment of the samples, we use a white light source with direct current (dc) power supply (Edmund Optics) for illumination from the top to avoid any interference from changing light intensity in the ionic current measurements. We use a pellicle beam splitter [PS in Fig. 1(a), 92% transmission, 8% reflection, Edmund Optics], a lens [L3 in Fig. 1(a), $f=17.5$ cm, Newport], and a progressive-scan charge coupled device (CCD) camera (TM-6710, Pulnix) that is protected from infrared and red laser light by a broadband IR filter [Filter 2 in Fig. 1(a), Schott glass KG3, Melles Griot] and a short pass filter [Filter 2 in Fig. 1(a), cutoff wavelength 600 nm, Thorlabs], respectively. The images from the CCD camera can be streamed to the hard drive of the measurement computer via a camera link connection (NI PCI-1428, National Instruments).

IV. IONIC CURRENT DETECTION

For the ionic current measurements we use a commercial patch-clamp amplifier (Axopatch 200B, Axon Instruments) in resistive mode. The contact to the solid-state nanopore is established via two agarose salt bridges and platinum wires in two separate compartments filled with 1 M KCl and 0.01 M ferri/ferro-cyanide (Sigma) as the redox species. These are needed to fix the potential of the platinum wires with respect to the liquid and to reduce the resistance of the Pt-wire interface to a few kΩ. The noise in the ionic current detection is primarily determined by the diameter of the hole in the polydimethylsiloxane (PDMS) layer and thus by the capacitance of the silicon chip containing the nanopore.

V. DATA ACQUISITION

The data acquisition (DAQ) for the ionic current measurements, the position detector, and the CCD camera is carried out by custom-written LabView software (LabView 7.0, National Instruments) that allows the user to simultaneously record all signals with a maximum sampling frequency of 40 kHz for each channel and at a video rate of 120 frames/s. The voltage applied across the nanopore is controlled by the analog outputs of the National Instruments card by using the internal voltage source of the Axon amplifier. The maximum available voltage ranges from −1.0 to 1.0 V. Using the TTL output of the DAQ card, we also control an electronic shutter (Melles Griot) that can shut off the IR laser as needed.

VI. FLOW CELL

It is quite challenging to construct a flow cell that has a low volume while incorporating an optical window that allows light to be focused onto the nanopore. The low volume is especially desirable for future experiments in which proteins will be added to one side of the nanopore. A cross section through the assembled cell is shown in Fig. 1(c). First, we make the lower part of the flow cell from PDMS layers (Sylgard 184, Dow Corning) with the outline shown in Fig. 1(b). The width of the channels is 300 μm and the height is 100 μm [Fig. 1(b)]. We include two entrance channels and one exit channel. The layers have a total thickness of 150 μm. The thickness of the layer has to be lower than the working distance of our objective of 200 μm to ensure good image quality and optical trapping. The total volume of our PDMS channels is only ~1 μl, which is an advantage when using biological samples that are usually only available in small quantities. The beads are flushed through the PDMS channels below the chip containing the nanopore [see Fig. 1(c)].

The PDMS layers are made using a mold that is micromachined in aluminum. The mold can be reused and is easily cleaned. Curing of the PDMS is done at 150 °C in a commercial oven for 10 min. For bonding of the PDMS layers to glass substrates, we clean glass slides (Menzel Gläser, 22 mm × 22 mm, thickness 0.2 mm) in an ultrasound bath for 10 min in acetone and 10 min in isopropanol. The PDMS is then exposed to an oxygen plasma for 30 s and directly positioned on the glass slides. Good covalent bonding between glass and PDMS is improved by performing this process within 2 h of the curing process. The best results in terms of sealing of the channels were obtained by letting the freshly made cells rest for a few days. After usage, the layers can be cleaned in methanol in an ultrasound bath. However,

after two of these cleaning steps, the layers should not be reused because of residues from previous experiments.

In the center of the main channel, a small hole is made with a sharpened injection needle to access the nanopore [Fig. 1(b)]. The typical diameter of the hole is 400–800 μm. This size allows manual alignment of the nanopore chip with the hole and also sets the capacitance of the chip that partly determines the noise in the current measurements.

The cell is assembled as follows. First we place the nanopore chip containing a single pore on top of the PDMS/glass layer with the membrane aligned to the center of the hole. The nanopore chip is held in place by a custom-made perspex block that creates a reservoir on top of the chip. Perspex is transparent and allows illumination of the sample from the top. Sealing is established with a small O-ring with an inner diameter of 2.1 mm [Fig. 1(c)]. The buffer in the top compartment can be refreshed by two channels with a diameter of 400 μm leading to and from the chip. The use of standard connectors (Upchurch Instruments) enables the connection with Teflon tubing (Upchurch Instruments) for the flushing of buffer solutions. The perspex block is connected to a baseplate with four screws that allow for adjustment of the applied pressure to establish the seal of the PDMS channels and the parallel mounting of the chip with respect to the piezo x,y-coordinate system. The baseplate is made from polyetheretherketone (PEEK) and acts as support for the PDMS/glass compound. The PEEK baseplate has a 8 mm diameter opening for the objective [indicated in Fig. 1(c)]. This allows enough movement for the objective and provides support to seal the cell without breaking the glass slide supporting the PDMS layer with the nanopore chip. After the completed assembly, the cell is flushed with buffer by simple manual pipetting of the solutions. Our design allows assembly and testing of the flow cell with the nanopore before it is mounted onto the microscope. All parts except the PDMS channels are cleaned prior to and after the experiments by sonicating for 20 min in a soap solution followed by thorough washing with de-ionized water and another 20 min sonication in ethanol.

After checking for trapped air bubbles in the PDMS channel, the filled cell is mounted on top of a three-axis piezoelectric stage with closed-loop capacitive position feedback (P-517.3CL, scan range x,y axis: 100 μm, z axis: 20 μm, Physik Instrumente). The piezostage is set on 2 micometer-stages (Newport) that allow coarse movement of the sample in x,y to align the nanopore membrane with the microscope objective. A small Faraday cage [thick dashed lines in Fig. 1(a)] encloses the piezostage and blocks outside interference by electromagnetic radiation with the ionic current measurements. After mounting of the flow cell the salt bridges are added and the setup is ready to use.

VII. CHARACTERIZING NANOPORES

We start the experiments by checking the current-voltage (I-V) characteristics of the nanopore. A good nanopore exhibits a linear I-V curve. In Fig. 2 we show several I-V curves for nanopores with diameters 6 nm (red dots), 10 nm (green triangles), and 20 nm (black squares). As expected,

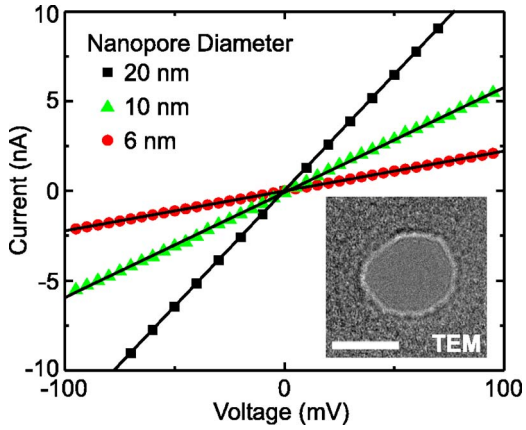

FIG. 2. (Color online) Current as a function of voltage for three nanopores in 1 M KCl. The diameters are 20 nm (black), 10 nm (green), and 6 nm (red). The points denote the measured data and the black lines are linear fits to the data. Inset: TEM image of a typical nanopore. The scale bar is 10 nm.

we observe that with increasing diameter the conductance and thus the gradient of the I-V curves increases. The solid black lines are linear fits to the measured data (Fig. 2). A nanopore with a linear I-V curve usually also has a very stable ionic current at fixed voltage that stays constant for hours or even days. In our experience, nanopores with these characteristics are especially suited for voltage-driven DNA translocation. Nanopores with nonlinear and/or rectifying characteristics[20,21] are not used for experiments discussed here, although we occasionally encounter them.

VIII. LOCALIZING THE POSITION OF NANOPORES

The next step is localizing the nanopore position on the membrane. Our thin membranes (20–60 nm thickness) containing the nanopores usually have a diameter of 5 μm. A typical example of the optical image of a membrane is shown in Fig. 3(a). The round membrane has a diameter of 5 μm and the nanopore is usually situated near the center. Please note that one pixel in this image has an area of roughly 100 times the area of a 10 nm diameter nanopore.

The method is summarized in Fig. 3(b). As described in detail elsewhere,[22] the infrared trapping laser locally heats the liquid which absorbs partly the power in the laser focus. This leads to a decreased resistivity ρ_{KCl} of the KCl solution. Since the resistance R of the nanopore is linearly proportional to ρ_{KCl}, we obtain a peak in the ionic current by scanning the infrared laser through the nanopore. This peak denotes the temperature profile created by the absorbed laser power in the water and can be used to measure the point-spread function of a microscope objective.[22] Alternatively, using this scanning we can also detect the position of the nanopore by scanning the laser focus of the infrared laser over the membrane and simultaneously measuring the ionic current.

A typical two-dimensional (2D) scan of the ionic current is shown in Fig. 3(c) for a 17 nm diameter nanopore. The conductance is shown as color scale where red denotes high, white medium, and blue low conductance. We observe a peak in the conductance at the nanopore position. Figure 3(d) shows a similar 2D conductance scan for a nanopore located

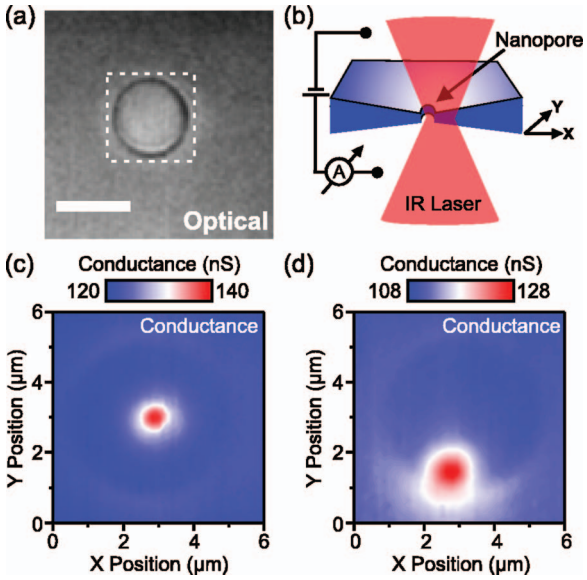

FIG. 3. (Color) (a) Image of the round membrane (diameter 5 μm) containing a single nanopore taken by the CCD camera. (b) The tightly focused IR laser is scanned across the nanopore and the ionic current through the nanopore is measured. (c) Resulting 2D conductance map as a function of the x, y position of the laser. The scanned area is indicated by the dashed line in (a). The nanopore (diameter 15 nm) was drilled near the center of the membrane. The peak indicates the position of the nanopore. (d) 2D conductance map of another nanopore (diameter 18 nm) that was drilled at the edge of the membrane. This shows that the conductance peak reliably corresponds to the nanopore position.

near the edge of the membrane. With this simple technique, nanopores can be accurately located in an optical microscope without any further modifications. By fitting the peak with a 2D Gaussian we can localize the nanopores with an accuracy of 20 nm with respect to the edge of the membrane. This is remarkable since localizing a nanopore would require tagging with fluorescent dyes, measuring the scattered light from the nanopore edge in an optical microscope, or using scanning ion conductance microscopy.[23,24]

IX. DETERMINATION OF OPTICAL TRAP-NANOPORE DISTANCE

We use the capacitive feedback of the piezoelectric stage to measure and control the distance between the nanopore and the optical trap. The accuracy of the capacitive feedback is better than 1 nm. However, the heat deposited in the flow cell leads to some drift because of thermal expansion. We correct for this temperature-induced drift by using a simple trick that allows one to obtain the distance between the nanopore and the optical trap with optical means. The round membrane [Fig. 3(a)] containing the nanopore has a diffraction pattern that depends on the distance between the objective focus and the membrane. We can use this pattern to independently determine the absolute distance between optical trap and nanopore, very similar to techniques used in, e.g., magnetic tweezers.[25] This is done by recording the diffraction pattern as a function of separation between objective focus and membrane. This z-calibration table is used to measure the distance between the membrane and the bead by simply comparing the diffraction pattern measured with the CCD camera with the lookup table. Here, the diameter of the membrane containing the nanopore is crucial and deliberately set to be 5 μm for our beads of 2 μm diameter. If the membrane had a smaller diameter, the diffraction pattern from the trapped bead would interfere with the pattern from the membrane, making this type of position determination impossible. The diameter of the membrane should be at least a factor of 2 larger than the diameter of the trapped bead. This allows measuring a clear diffraction pattern from the membrane even in the presence of a bead in the optical trap. Due to limitations of our illumination and camera setup [most of the light (90%) is used for the quadrant PD] the resolution is modest and lies around ~50 nm. However, this is more than sufficient to function as an independent measure for the distance between nanopore and optical trap.

X. DNA-BEAD CONSTRUCTS

After checking the electrical properties and localizing the nanopore, beads are injected through the side channel [Fig. 1(b)]. We trap a single bead in the focal spot of the optical tweezers below the nanopore as indicated in Fig. 1(c). The other beads are then removed by flushing at least another 5 μl of buffer through the main channel. We use pressure generated by custom-made micrometer screws that push the piston of the syringes containing the solutions [see Fig. 1(a)]. For the trapping experiments we use polystyrene particles coated with streptavidin (diameter ~2 μm, Polysciences). The DNA for the experiments is made by standard molecular biology techniques and end labeled with a single biotin molecule. The DNA is bound to the beads prior to the measurements. We wash 5 μl of bead solution twice in 10 mM Tris-HCl 0.1 mM EDTA(TE)-buffer (Sigma) containing 50 mM KCl. The beads are then reimmersed in 2 M KCl with 10 mM TE and typically mixed with 5 μl of DNA solution (concentration 5–10 ng/μl). The exact quantities depend on the specific concentrations of beads and DNA. We usually aim for a ratio of 100:1 between DNA and beads to ensure binding of multiple DNA molecules. The beads are incubated with the DNA for 15 min and then washed again with 10 mM TE buffer and 50 mM KCl. Afterwards, the DNA-bead constructs are suspended in the desired measurement buffer. We use one of the following measurement buffers: between 10 mM and 100 mM KCl we use 1 mM TE-Buffer, for 100 mM KCl–1 M KCl we use 10 mM TE buffer. We add 0.1% polyoxyethykenesorbitan monolaurate (Tween20, Sigma Aldrich) to all measurement buffers, in order to reduce sticking of the beads to the surface. We usually dilute the solution with the DNA-bead constructs with buffer solution by a factor of 1000 and obtain in total 2–3 ml of measurement buffer, allowing multiple experimental runs with one buffer preparation. The buffer can be stored in the fridge at 4 °C for up to 3 days, but clustering of beads is often observed already after 24 h.

XI. TRAP CALIBRATION

After trapping a single bead, a calibration of the optical trap is performed by recording several power spectra. A typical example is shown in Fig. 4(a) for incident laser powers of

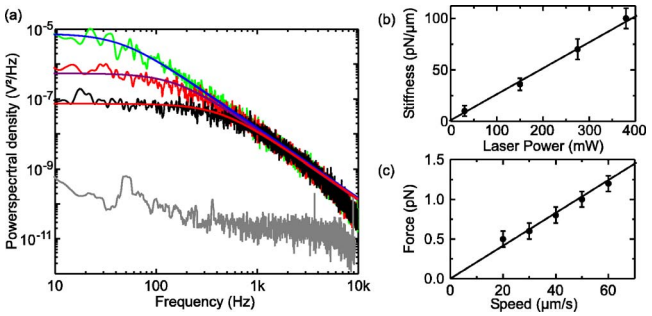

FIG. 4. (Color online) (a) Power spectral density as a function of frequency for the optical trap at 150 mW (green), 270 mW (red), and 380 mW (black). The lowest (gray) curve is the background for an empty trap. The drop at 8 kHz is due to the high frequency cutoff of the electronics. The data was sampled at 45 ksamples/s. (b) Trap stiffness as a function of incident laser power. The stiffness is calculated using the Stokes drag and the corner frequency of the power spectra in (a), as described in the text. (c) Measured drag force on a bead with 2.2 μm diameter as a function of piezo speed (trap stiffness 3 pN/μm). The points are the experimental data, and the line denotes the calculated drag force on a 2.2 μm bead.

150, 275, and 380 mW, as measured in front of the back aperture of the objective. The gray curve in Fig. 4(a) is the background signal when no bead is trapped.

The fits to the data (solid lines) in Fig. 4(a) are calculated with the Lorentzian function that describes the response of a particle in an harmonic potential[26] in the presence of Brownian noise:

$$S(f) = \frac{k_B T}{\beta \pi^2 (f^2 + f_c^2)}, \tag{1}$$

where f is the frequency, f_c is the cutoff frequency, $k_B T$ is the thermal energy of the system, and $\beta = 6\pi\eta r$ is the drag coefficient of the bead where η denotes the viscosity of the liquid and r is the bead radius.[26] The trap stiffness κ is then simply calculated from the cutoff frequency f_c using $\kappa = 2\pi\beta f_c$. We find a linear dependence of the trap stiffness on the incident laser power [Fig. 4(b)], as expected. The calibration is verified by measuring the drag force on the trapped bead. For this, we move the bead at a known speed through the liquid using our calibrated piezostage. A typical result is shown in Fig. 4(c) for a low trap stiffness of $\kappa = 3$ pN/μm.

Following the calibration procedure, we check if the bead nonspecifically sticks to the membrane by pushing it against the surface for a few seconds. In most cases, the bead can be pulled easily off the surface. We found that a small amount of surfactant like Tween20 in the measurement buffers reduces unwanted sticking of the bead to the surface.

XII. CAPTURE AND CONTROL OF DNA IN THE NANOPORE

After this last check of the integrated system, experiments can be conducted. In the following we will show that we can control the number of DNA molecules in the nanopore and the amount of the tethered DNA on both sides of the nanopore.

DNA can be captured in the nanopore by bringing the bead close (down to 1 μm surface to surface) to the membrane. The probability for capture of DNA in the nanopore is determined by the amount of DNA on the bead and the distance between the bead surface and the nanopore. We tether tens of DNA molecules to the 2 μm diameter beads to create a high local concentration around them. The capture probability is enhanced when the distance between bead-surface and nanopore is lower than twice the radius of gyration R_g of the DNA. In our case for λ-DNA with $R_g \sim 500$ nm, we can work with a typical nanopore bead distance of 1–2 μm. This also ensures that the bead stays far away from the surface to avoid unwanted sticking. The typical waiting time between captures can be easily tuned with the choice of these parameters to lie between seconds (bead-nanopore distance within $2R_g$) and hours (bead-nanopore distance above $10R_g$).

A higher voltage applied across the nanopore leads also to more frequent capture events. From our experience, the voltage should lie between 30 and 100 mV. This also limits the danger that the streptavidin-biotin bond is broken and the DNA is no longer tethered to the trapped bead. Breakage of the bond can especially occur when voltages exceeding 150 mV are applied over the nanopore.

The salt concentration in the buffer determines both the conductance of the nanopore and the conductance change when a DNA molecule is in the nanopore.[18] At a salt concentration of 0.1 M KCl the typical conductance of a 10 nm diameter nanopore lies around 10 nS.[18] At this concentration, the presence of DNA in the nanopore leads to an increase in conductance of $\sim 0.5-1$ nS.[18] We typically set the internal Bessel filter of our current amplifier to 1 kHz to obtain a sufficiently high signal-to-noise ratio. This enables the counting of single DNA molecules as they enter the nanopore. Figure 5 shows the real-time capture of tethered DNA molecules in a nanopore with 13 nm diameter. The current is plotted as a function of time while the voltage is varied between $V = -100$ and 100 mV. For this measurement, the distance between the bead center and the nanopore was 3 μm. The large steps and the spikes in the measurement are caused by switching the voltage across the nanopore. The voltages at every plateau are also shown in Fig. 5. At the first plateau ($V = 50$ mV) no DNA is present in the nanopore. After switching the voltage to $V = 100$ mV at $t = 2.5$ s, we observe an abrupt increase of the conductance at constant voltage, as indicated by the black arrow. At this moment a single DNA molecule has entered the nanopore and remains stalled there due to the opposing force on the attached bead held in the optical trap. The number of DNA molecules in the nanopore is indicated by the numbers on top of the graph. (0) denotes that no DNA is present in the nanopore and (1) that one molecules is in the nanopore [see the lower part of Fig. 5 for sketches of cases (0) and (1)].

At this positive voltage an untethered DNA molecule would translocate through the nanopore in a few ms.[18] In contrast, our tethered DNA does not fully traverse the nanopore but is held by the bead in the optical trap. Parts of the DNA are now present on both sides of the membrane, as indicated by the sketches below the data in Fig. 5. As a consequence we observe only a step in the ionic level and not a short transient blockade for free DNA. We can now hold a single molecule in the nanopore for several hours.

We verify that we can also drive the DNA out of the nanopore by reversing the sign of the voltage ($V = -100$ mV,

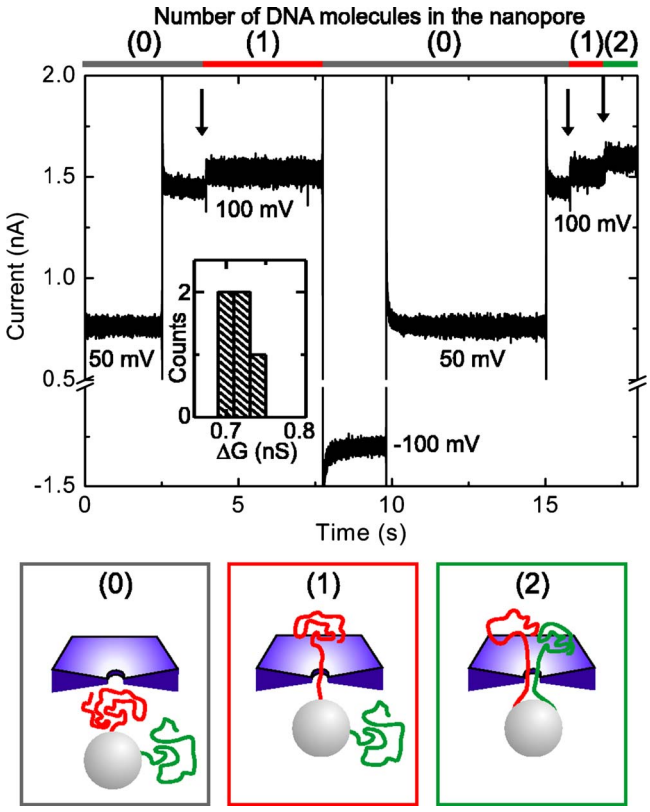

FIG. 5. Monitoring the ionic current through a nanopore (13 nm diameter) as a function of time in 0.1 M KCl to detect the capture of tethered DNA molecules. The applied voltages are, as a function of time, $V=50$, 100, -100, 50, 100 mV. The arrows denote a capture of a single DNA molecule in the nanopore, indicated by the increased current through the nanopore. The number of molecules in the nanopore is given by the numbers on top of the graph. The colors correspond to the sketches shown below the graph for a nanopore containing (0), (1), or (2) DNA molecules. Please note that we have numerous DNA molecules bound to the bead but we sketch only two for simplicity. The inset shows a histogram for the change in conductance ΔG for DNA captures observed with this nanopore.

$t=7.5$ s). This is successfully accomplished as indicated by the subsequent current plateau at $V=50$ mV where we recover the original current value of the empty nanopore. We then increase the voltage to $V=100$ mV and this time observe two sharp steps upwards in the current. This indicates the entry of two new DNA molecules into the nanopore in rapid succession. The nanopores now contains two molecules [see sketch (2) in Fig. 5]. In the inset of Fig. 5 we show a histogram of conductance changes ΔG observed in this experiments. All events are centered around 0.75 nS, which overlaps very nicely with data obtained with untethered DNA.[18] In most cases we observe that the DNA enters the nanopore in an unfolded state.[5,27] Obviously, the number of DNA molecules in the nanopore can be easily tuned by driving DNA out again with the voltage and changing the distance between nanopore and optical trap or as explained above.

These experiments clearly demonstrate several achievements and solved the technological question we started with. First we can detect DNA entering the nanopore. Second, our current resolution is good enough to exactly count the number of DNA molecules in the nanopore. Last and most importantly, we can arrest a DNA molecule in a nanopore.

XIII. FORCE MEASUREMENTS

Having established the controllable presence of single DNA molecules in the nanopore, we can now measure the force exerted by the electrical field on a tethered DNA molecule simply by monitoring the position of the bead in the optical trap. The force measurements are performed along the optical axis or z direction of the piezoelectric stage. Our measurements critically depend on the relative position of the trap and the circular membrane shown in Fig. 3(a). We typically align the bead directly above the nanopore with an accuracy only limited by the resolution of the x,y-detection system to avoid any artifacts when the bead is not pulled parallel to the optical axis by the DNA molecule. The measurements are then performed as follows. With a single DNA molecule in the nanopore we continuously extend the distance between the bead and the nanopore with the piezoelectric stage over several microns. For this we use a very low voltage of 10 mV across the nanopore and a typical piezo speed of 50 nm/s. This is several orders of magnitude slower than the normal translocation speed of 16 mm/s observed with solid-state nanopores[18] and the speed of 0.12–0.4 mm/s measured for single-stranded DNA through protein nanopores like α-hemolysin.[28] In fact, we are able to pull the DNA fully out of the nanopore against the electrical field by using the mechanical force exerted with the optical trap[29] and we accurately control the length of the DNA molecule on both sides of the nanopore.

A typical example for such measurements is shown in Fig. 6. We plot the PD sum signal as a function of separation between trap center and nanopore (continuous dark gray line). For simplicity we refer to this as the "bead position" in the following. The oscillating behavior stems from the interference of the reflected light from the bead and the membrane containing the nanopore. Please note that the nanopore is on the left of this graph at position 0. The exact distance of the trap from the nanopore is checked by using both the feedback of the piezostage and the diffraction pattern of the round membrane. During the following experiments, the DNA molecule is not fully pulled out of the nanopore because the distance between the nanopore and optical trap remains at all times lower than the DNA contour length and the voltage remains positive.

For the force measurements, we apply a given positive voltage for a few seconds. This pulls the DNA, and hence the bead, toward the nanopore. The PD signal is measured at each corresponding voltage change for 1–2 s to obtain a good signal-to-noise ratio. The photodiode response is then averaged and plotted onto the calibration curve taken earlier (Fig. 6, dark gray, full line). The results of seven such measurements are shown in Fig. 6 by points in different colors. Each collection of points shows an individual measurement where the distance between the bead and the nanopore is first set using the piezoelectric stage and then decreased again by increasing the force on the DNA molecule in the nanopore through the application of a higher voltage. For each set distance between bead and nanopore, we varied the voltage in a stepwise fashion between 10 and 100 mV (step size 10 mV) with the same DNA molecule in the nanopore. The

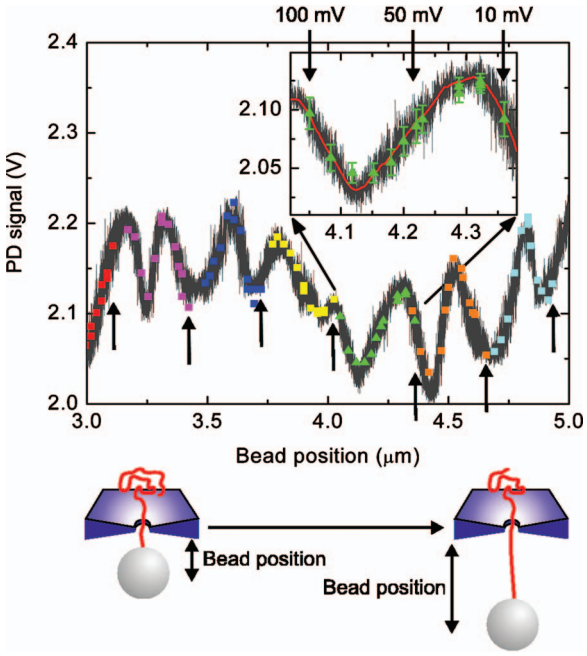

FIG. 6. (Color) Signal of the red laser on the quadrant PD as a function of distance between the bead and the nanopore. The full dark gray curve shows the calibration of the detector response when we continuously increase the nanopore-bead distance. The points indicate the position of the bead when we select a certain starting point and subsequently apply voltages between 10 and 100 mV across the nanopore. Within each series of different colored points, the rightmost denotes low voltage (10 mV, low force) and leftmost point high voltage (100 mV, high force) on the DNA molecule. The lower sketch shows the bead position for the leftmost data set (red squares) and the rightmost data (light-blue squares). The inset shows a magnification of a single measurement in which a series of voltages are applied (green triangles). The red line is the averaged signal used for position detection of the bead.

starting and finishing position for the individual measurements is marked in Fig. 6 by the vertical arrows. This data shows that we can accurately measure the bead position for bead-membrane separations of up to 5 μm.

The accuracy of the position detection is further demonstrated with the inset of Fig. 6 where we depict a zoom on one of the measurements (green triangles). The red line is the averaged signal of the calibration data. The green triangles denote the PD voltages that we measure at different voltages across the nanopore. The distance of the bead from the center of the trap can now be easily obtained by comparing the starting position marked by the arrow at low voltages with the position of the bead at high voltages. Again, the nanopore is on the left of this graph at position 0. We observe a deviation between the measured data and the calibration curve of less than 1 nm to up to 10 nm. With the trap stiffness of 50 pN/μm in this measurement, we obtain a force resolution 0.05–0.5 pN. From the distance between the first and last point of the measurements we can directly calculate the force on the DNA molecule to be 23 ± 2 pN/mV. The error here is not limited by the force resolution but rather by the uncertainty of the drag coefficient of the bead with the attached DNA molecules and the calibration of the optical trap.

XIV. CONCLUSION

We have developed a novel experimental technique that combines optical tweezers with ionic current detection and solid-state nanopores. We have demonstrated that we can localize single nanopores with an optical microscope by using a highly focused infrared laser as local heat source. Our results show that we are able to controllably insert single DNA molecules into an individual nanopore. We show that high accuracy position measurements are possible by using the reflected light from the bead and the membrane. With our new apparatus with single nanometer resolution, we are able to arrest DNA molecules in nanopores and we can measure the force on this DNA molecule. Our new setup makes this very important quantity directly experimentally accessible. In addition, we believe that our new combination of nanopores and optical tweezers can be used for new experiments in biophysics like the theoretically proposed unzipping of RNA hairpins[14,15] and the detection of proteins bound to DNA.[13] This setup is also well-suited to address a multitude of questions concerning the physics of polymers in confined geometries.

ACKNOWLEDGMENTS

We would like to thank Bernard Koeleman and Stijn van Dorp for assistance in taking data and making the PDMS layers, and Peter Veenhuizen, Suzanne Hage, and Ya-Hui Chien for help with the biochemistry. The nanopores were made by Diego Krapf, Ralph Smeets, and Meng-Yue Wu. Finally, we acknowledge useful discussions with Derek Stein, Diego Krapf, Bernadette Quinn, Ralf Seidel, and Daniel Koster. This work was financially supported by FOM and NWO.

[1] J. J. Kasianowicz, E. Brandin, D. Branton, and D. W. Deamer, Proc. Natl. Acad. Sci. U.S.A. **93**, 13770 (1996).
[2] A. Meller, L. Nivon, E. Brandin, J. Golovchenko, and D. Branton, Proc. Natl. Acad. Sci. U.S.A. **97**, 1079 (2000).
[3] J. Li, D. Stein, C. Mcmullan, D. Branton, M. J. Aziz, and J. A. Golovchenko, Nature **412**, 166 (2001).
[4] A. J. Storm, J. H. Chen, X. S. Ling, H. W. Zandbergen, and C. Dekker, Nat. Mater. **2**, 537 (2003).
[5] A. J. Storm, J. H. Chen, H. W. Zandbergen, and C. Dekker, Phys. Rev. E **71**, 051903 (2005).
[6] J. A. Schellman and D. Stigter, Biopolymers **16**, 1415 (1977).
[7] G. S. Manning, Q. Rev. Biophys. **11**, 179 (1978).
[8] G. S. Manning and J. Ray, J. Biomol. Struct. Dyn. **16**, 461 (1998).
[9] J. L. Viovy, Rev. Mod. Phys. **72**, 813 (2000).
[10] G. W. Slater, C. Desrulsseaux, S. J. Hubert, J. F. Mercier, J. Labrie, J. Boileau, F. Tessier, and M. P. Pepin, Electrophoresis **21**, 3873 (2000).
[11] C. Bustamante, Z. Bryant, and S. B. Smith, Nature **421**, 423 (2003).
[12] K. C. Neuman and S. M. Block, Rev. Sci. Instrum. **75**, 2787 (2004).
[13] S. J. Koch and M. D. Wang, Phys. Rev. Lett. **91**, 049903 (2003).
[14] U. Gerland, R. Bundschuh, and T. Hwa, Phys. Biol. **1**, 19 (2004).
[15] R. Bundschuh and U. Gerland, Phys. Rev. Lett. **95**, 208104 (2005).
[16] D. Krapf, M. Y. Wu, R. M. M. Smeets, H. W. Zandbergen, C. Dekker, and S. G. Lemay, Nano Lett. **6**, 105 (2006).
[17] M. Y. Wu, D. Krapf, M. Zandbergen, H. Zandbergen, and P. E. Batson, Appl. Phys. Lett. **87**, 113106 (2005).
[18] R. M. M. Smeets, U. F. Keyser, D. Krapf, M. Y. Wu, N. H. Dekker, and C. Dekker, Nano Lett. **6**, 89 (2006).
[19] G. V. Shivashankar, G. Stolovitzky, and A. Libchaber, Appl. Phys. Lett. **73**, 291 (1998).
[20] Z. Siwy, E. Heins, C. C. Harrell, P. Kohli, and C. R. Martin, J. Am. Chem. Soc. **126**, 10850 (2004).
[21] Z. Siwy, I. D. Kosinska, A. Fulinski, and C. R. Martin, Phys. Rev. Lett. **94**, 048102 (2005).
[22] U. F. Keyser, D. Krapf, B. N. Koeleman, R. M. M. Smeets, N. H. Dekker, and C. Dekker, Nano Lett. **5**, 2253 (2005).

[23] Y. E. Korchev, C. L. Bashford, M. Milovanovic, I. Vodyanoy, and M. J. Lab, Biophys. J. **73**, 653 (1997).
[24] Y. E. Korchev, Y. A. Negulyaev, C. R. W. Edwards, I. Vodyanoy, and M. J. Lab, Nat. Cell Biol. **2**, 616 (2000).
[25] T. R. Strick, J. F. Allemand, D. Bensimon, A. Bensimon, and V. Croquette, Science **271**, 1835 (1996).
[26] F. Gittes and C. F. Schmidt, Methods Cell Biol. **55**, 129 (1998).
[27] J. L. Li, M. Gershow, D. Stein, E. Brandin, and J. A. Golovchenko, Nat. Mater. **2**, 611 (2003).
[28] D. W. Deamer and D. Branton, Acc. Chem. Res. **35**, 817 (2002).
[29] U. F. Keyser, B. N. Koeleman, S. van Dorp, D. Krapf, R. M. M. Smeets, S. G. Lemay, N. H. Dekker, and C. Dekker, Nature Phys. **2**, 473 (2006).